Nanoscale

Au@Ag core/shell nanoparticles as a colorimetric probe for cyanide sensing

Journal:	*Nanoscale*
Manuscript ID:	NR-COM-05-2014-002560.R1
Article Type:	Communication
Date Submitted by the Author:	17-Jun-2014

Complete List of Authors:	Zeng, Jingbin; College of Science,China University of Petrolem, Chemistry Cao, Ying-ying; China university of Petroleum, Chen, Jingjing; China university of Petroleum, Wang, Xu-dong; Institute of Biological Interface, Karlsruher Institut für Technologie; Universität Regensburg, Institut für Analytische Chemie, Chemo- und Biosensorik, Yu, Jianfeng; China University of Petroleum (East China), Department of Chemistry, College of Science Yan, Zi-Feng; China University of Petroleum, School of Chemical Engineering Chen, Xi; Xiamen University, Chemistry

Journal Name

RSCPublishing

COMMUNICATION

Au@Ag core/shell nanoparticles as a colorimetric probe for cyanide sensing

Cite this: DOI: 10.1039/xoxxoooooox

Jing-bin Zeng[a,*], Ying-ying Cao[a], Jing-jing Chen[a], Xu-dong Wang[b], Jian-feng Yu[a], Bin-bin Yu[c], Zi-feng Yan[a], Xi Chen[d]

Received ooth January 2012,
Accepted ooth January 2012

DOI: 10.1039/xoxxoooooox

www.rsc.org/

We synthesize Au@Ag core-shell nanoparticles (NPs) using Au NPs assisted Tollens reaction. The as-synthesized NPs are used for the colorimetric cyanide sensing with a detection limit of 0.4 μM. The colorimetric system is immobilized into argrose gels as portable "test strips".

Cyanide anion is highly toxic to mammals, since it can strongly bind with Fe^{3+} of heme cofactors in a_3 cytochrome to rapidly deactivate its oxygen transport function.[1] Nevertheless, cyanide is widely used in several industrial activities, particularly in electroplating, metallurgy and organic polymer production,[2] which raises the risk of its contamination to environmental water. A variety of receptors or sensors has been developed to bind or sense cyanide.[2-4] These chemosensors are based on either an organic chemophore or metal complex, which reacts or coordinates with cyanide to induce spectral changes.[6, 7] Despite the good sensitivity and selectivity obtained for cyanide, drawbacks such as laborious organic synthesis,[6a-c, 7c] poor water compatibility [6e-h] and/or long reaction time, limit their practical application.

Cyanide is able to dissolve metals like gold and silver in the presence of oxygen via the formation of metal-cyanide complex.[8] Taking advantage of this property, a number of gold (Au) and silver (Ag) nanoparticles (NPs) based fluorescent probes have been explored for cyanide sensing.[9] For instance, cyanide can induce the dissolution of dye-adsorbed Au NPs, which enables a sensitive "turn-on" fluorescent detection of cyanide.[9b, c] These approaches allow the detection of cyanide in pure aqueous medium with high sensitivity, but rely on specialized equipment and considerable skills. Therefore, development of a simple, rapid, sensitive and selective sensing system that allows the visual readout of cyanide in real samples is still highly imperative.

The surface plasma resonance (SPR) of Au@Ag core/shell nanostructures is highly dependent on the dimensional shell-to-core ratio,[10] and therefore its slight variation often leads to an obvious spectral and/or color change. This property prompts us to develop a cyanide detection approach based on Au@Ag core/shell NPs, since cyanide is expected to be able to modify the dimensional shell-to-core ratio by sequentially dissolving silver shells and gold cores as shown in Scheme 1 and as a result, one can tune the absorption spectra shape. The corresponding apparent color changes are also in direct relation to the cyanide concentration, and thus can be utilized for colorimetric detection of cyanide.

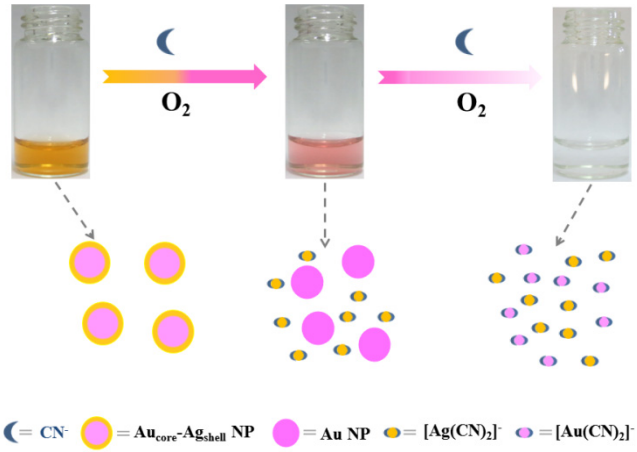

Scheme 1. Schematic diagram of the Au@Ag core/shell NPs for the colorimetric detection of cyanide.

The Au@Ag core/shell NPs were synthesized using citrate capped Au NPs coupled with the classic Tollens reaction, in which the silver nanoshells generated from the Tollens reaction deposited over the Au NPs.[11] Fig. 1a-c reveal that most of bimetallic NPs were spherical and exhibited electronic inhomogeneity with a dark core surrounded by a lighter shell. An overlay of energy-dispersive X-ray spectroscopic (EDX) maps on a representative bimetallic NP (Fig. 1d) indicates the presence of gold and silver element, which primarily located at the central and outer part, respectively. The size distribution histogram of the as-prepared Au@Ag core/shell NPs was given in Fig. S1, and their mean sizes were 21.8±2.5 nm. The zeta potential of the Au@Ag core/shell NPs was measured as -40.8

mV, which was similar to that of Au NPs (-43.8 mV). These results implied that the surface of Au@Ag core-shell NPs was also probably capped by the negative citrate, which can stabilize the NPs against aggregation with electrostatic repulsion.[12] The as-synthesized NPs can be stable within the pH ranging from 5-11 without aggregation (Fig. S2).

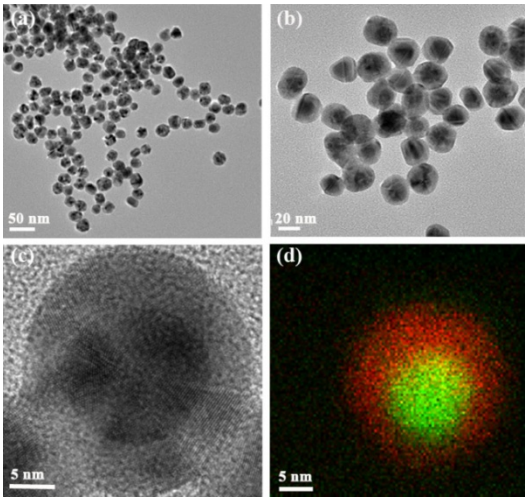

Fig. 1 (a, b) TEM images (c) a typical HR-TEM image and (d) an EDX elemental map shown as the overlay of Au and Ag signal of Au@Ag core/shell NPs.

In view of the sensing mechanism mentioned above, the performance of the colorimetric assay probably depends on the silver shell thickness, which is related to the concentration of Tollens reagent ($[Ag(NH_3)_2]OH$) and HCHO. As shown in Fig. S3, we prepared Au@Ag core/shell NPs with thicker shell by increasing the concentration of HCHO. Fig. S4 indicated that the core/shell NPs with thick silver shells were beneficial for the detection of cyanide with wide concentration range, but they suffered from low sensitivity and visual resolution. In contrast, the NPs with thin silver shells were sensitive for the detection of cyanide, but the tunable color range was narrow (Fig. S5). The optimum concentrations of $[Ag(NH_3)_2]OH$ and HCHO were found to be 0.24 and 0.96 mM respectively to prepare the core/shell NPs with average thickness of silver shells at 4.4 nm (Fig. S1).[13] The concentration of Au NPs is also an important factor that can affect the tunable color range of the assay, which was optimized to be 1.2 nM (data not shown). The pH effect on the colorimetric assay was investigated from 8-11, because cyanide tends to be converted into volatile HCN under acidic and even neutral conditions. It can be seen from Fig. S6 that the colorimetric assay exhibited the best sensitivity for cyanide at pH 9.

We then used the colloidal Au@Ag core/shell NPs for the detection of cyanide. With the addition of incremental concentration of cyanide, the color of the colloidal solution turned from yellow to orange, pink, and finally colorless (Fig. 2a), which enables a visual detection of cyanide using bare eyes. The lowest concentration of cyanide that can be visually distinguished was 1.2 μM, which is lower than 1.9 μM, i.e. the maximum allowable concentration of cyanide in drinking water regulated by the World Health Organization.[14] For comparison, monometallic Ag NPs and Au NPs were synthesized and used for cyanide detection. As shown in Fig. 2b and c, both of these nanoprobes were also applicable for colorimetric cyanide detection as reported elsewhere [15] but suffered from low visual resolution. The use of core/shell nanoparticles significantly increases the color gradient, and thus improves visual resolution. Fig. 2d shows that the absorbance at 394 nm (A_{394}) decreased as the increase of cyanide concentration, and there was a linear relationship between the ΔA_{394} and cyanide concentrations in the range of 0.4-100 μM. The lowest detectable concentration was 0.4 μM, which is comparable to or even lower than those of fluorescence-based methods (Table S1). Such high sensitivity of the method is ascribed to the fact that cyanide is extremely reactive to silver and gold, and so a small amount of cyanide can modify significantly the dimensional shell-to-core ratio of Au@Ag NPs, leading to an observable change in both apparent color and the shape of absorption spectra. Fig. S7 shows that the response time of the approach was less than one minute. The reproducibility of the method was satisfatory with the relative standard deviation less than 2.3% (Fig. S8).

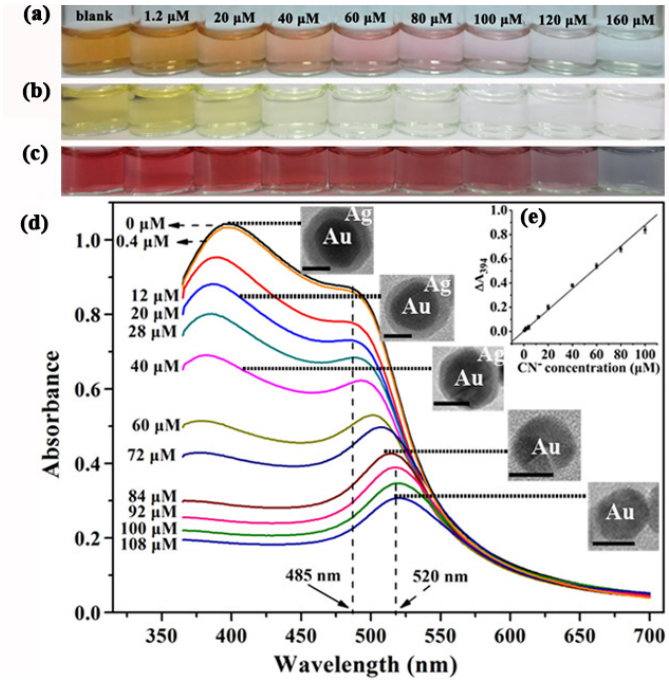

Fig. 2 Photographs of the (a) Au@Ag core/shell NPs (b) Ag NPs and (c) Au NPs with the addition of various amounts of cyanide; (d) UV-vis spectra of the Au@Ag core/shell NPs with the addition of increasing cyanide; Inset in Fig. 2d represents the corresponding TEM images of the Au@Ag core/shell NPs treated with different amounts of cyanide; The black scale bar represents the length of 10 nm; (e) linear plot of ΔA_{394} versus cyanide concentration.

To get insight on the mechanisms of the proposed approach, the spectra of the Au@Ag core/shell NPs with and without cyanide

treatment were correlated to their geometric dimension (Fig. 2b inset and Fig. S9). Fig. 2b shows that, as the cyanide concentration increasing from 0 to 40 μM, the intensity of high-energy SPR peak originated from silver shell continuously decreased, while the low-energy SPR peak belonging to gold core progressively red-shifted, indicating the dissolution of silver shell. TEM studies also reveal that the thickness of silver shells was decreased progressively from ~4.4 to ~2.8 and ~1.4 nm, while the size of gold cores remained almost constant. When the cyanide concentration reached 92 μM, the low-energy SPR peak disappeared and the high-energy SPR peak red-shifted to 520 nm, which is the typical plasmon resonance peak of Au NPs. The corresponding TEM image also revealed the disappearance of silver shell and the exposure of gold core. These results indicated that at the cyanide concentration of 92 μM, silver shells were completely dissolved, while the gold cores were thoroughly exposed but had barely been etched. As the cyanide concentration increased further, the low-energy SPR peak intensity continued to decrease but without any red shift, indicating the inceptive etching of gold cores. TEM studies also reveal that the size of Au NPs decreased from ~13.0 to ~12.1 nm when the cyanide concentration reached 108 μM. These findings demonstrate that cyanide progressively dissolved silver shell and gold core of Au@Ag core/shell NPs.

Inductively coupled plasma mass spectrometry (ICP-MS) was used to determine the silver and gold content in the Au@Ag core/shell NPs colloidal solution before and after cyanide treatment. High-speed centrifugation (16000 rpm) was used to precipitate the NPs, and the supernatant was collected for the analysis. As listed in Table S2, when the cyanide concentration increased from 0 to 92 μM, the silver and gold content increased from 0.29 to 7.0 mg L^{-1} and from 0.49 to 12.5 mg L^{-1}, respectively. Electrospray ionization time-of-flight (ESI-TOF) mass spectrometry was used to confirm the product generated by the reaction between Au@Ag core/shell NPs and cyanide. Fig. 3 shows that no gold- or silver-cyanide complex can be detected before cyanide treatment, while both of them were detected with the addition of increased cyanide. The two peaks appearing at m/z 158.92 and 160.92 belonged to $[Ag(CN)_2]^-$, while that of 248.98 corresponded to $[Au(CN)_2]^-$.

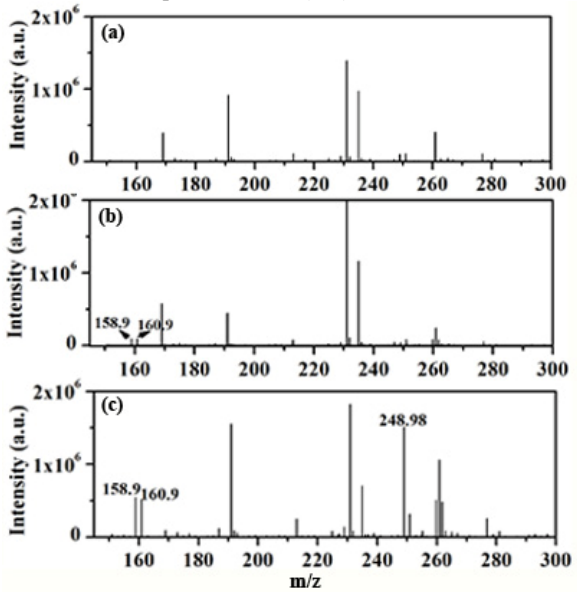

Fig. 3. The ESI-MS spectra for the supernatant of Au@Ag core/shell NPs with the addition of cyanide at (a) 0 (b) 8 and (c) 120 μM.

To examine the specificity of the approach, its response for cyanide as well as several other common anions and cations were investigated. Fig. 4 indicates that only the addition of cyanide into Au@Ag core/shell colloidal solution induced an apparent color change from yellow to pink and a significant decrease of absorbance at 394 nm. The coexistence of at least 25-fold excess of other anions (except the case of iodide) hardly affected the determination of cyanide. The mixture of the eighteen anions also has no significant effect on cyanide detection. Such good selectivity can be attributed to the unique reaction between cyanide and silver or gold as discussed above. The maximum interference was caused by one equiv. of iodide (80 μM), but the induced signal was still 9.2-fold lower than that of cyanide. Moreover, it must be emphasized that iodide concentration in natural water samples is always very low. For example, even sea water generally contains iodide at less than 1 μM.[9f] Fig. S10 shows that the responses induced by some common cations were at least 12.5-fold lower than that of cyanide. Furthermore, using EDTA as a masking agent, even 20 equiv. cations shows little interfering effect (Fig. S11).

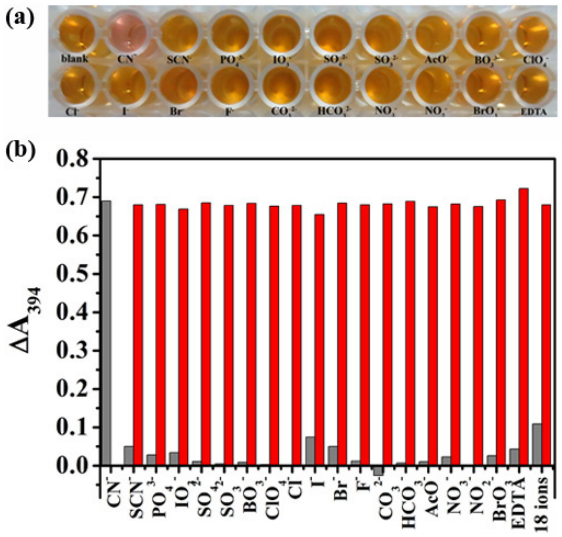

Fig. 4 (a) Photographs and (b) decreased absorbance at 394 nm (ΔA_{394}) of the Au@Ag core/shell NPs with the addition of different anions. Gray bars represent the ΔA_{394} of the Au@Ag core/shell NPs in the presence of different anions, red bars represent the ΔA_{394} of the Au@Ag core/shell NPs in the co-existence of cyanide and the other anion. The concentration was 80 μM for cyanide and iodide, 2 mM for phosphate and 4 mM for the other anions.

We immobilized the Au@Ag core/shell NPs into agarose gels and used them for the colorimetric detection of cyanide in aqueous medium. As can be seen in Fig. S12a, the colors of the agarose gels changed from yellow to orange, pink and finally colorless, which were very similar to those obtained in solutions. These agarose gels were directly used for UV-vis

analysis (Fig. S12b), and there was a linear relationship between the ΔA_{394} and cyanide concentration ranging from 8-80 μM (Fig. S12c). These results reveal the feasibility of the agarose gels for cyanide detection in terms of not only semi-quantitative colorimetric measurement but also quantitative determination. Nevertheless, it must be noted that the reaction process in the gel was much slower than that in the solution. This is probably due to the slower diffusion rate of cyanide ion in agarose gels. We further used these agarose gels for the analysis of natural samples including tap, sea, lake and industrial water samples. Fig. 5 shows that the agarose gels exhibited similar color changes from yellow to pink and colorless for ultrapure and the other natural water samples. It should be noted that all the samples are collected and directly analyzed without any pretreatment steps. These results demonstrated that the agarose gels were tolerant for the matrix effect from the natural water samples. By comparison, we found it is infeasible to use the Au@Ag core/shell solution for the direct analysis of industrial, lake and sea water samples, owing to its propensity to aggregation in the presence of high salinity.[16] Such disadvantage has been overcome by immobilizing the NPs system into agarose gel. In addition, initial results indicated that our agarose gels were also applicable to the analysis of gaseous hydrogen cyanide in the air (Fig. S13) and cigarette smoke (Fig. S14). Extensive studies on this research are still in progress.

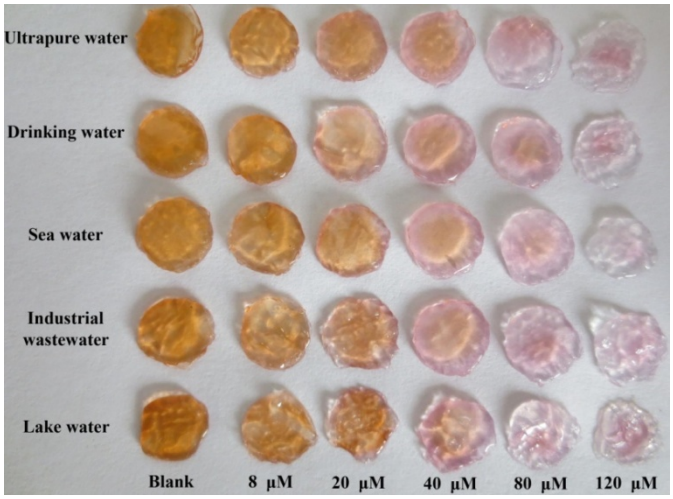

Fig. 5 Agarose gel "test strips" for the colorimetric detection of ultrapure, tap, sea, industrial, and lake water samples spiked with different concentrations of cyanide.

In summary, we propose a simple yet sensitive and selective cyanide detection approach by building Au@Ag core/shell nanostructures as a platform. The spectral behavior of Au@Ag core/shell NPs is highly dependent on the shell-to-core ratio, and thus highly sensitive to cyanide leaching and, more importantly, the concurrent induced color changes could be easily observed with bare eyes. We immobilize the Au@Ag core/shell NPs into agarose gels, which have realized the direct analysis of cyanide in natural water samples without sample pretreatment steps. This work could be further extended to other Au@Ag core/shell nanomaterials such as nanocubes and nanorods, which might also be applicable for the colorimetric sensing of cyanide with corresponding different color changes.

This work was financially supported by the National Nature Scientific Foundations of China (No. 21105123) and the Shandong Young Scientist Awards (BS2012CL037) which are gratefully acknowledged.

Notes and references

[a] State Key Laboratory of heavy oil processing and College of Science, China University of Petroleum (East China) ,Qingdao, 266555(China) E-mail: xmuzjb@163.com
[b] Institute of Analytical Chemistry, Chemo- and Biosensors University of Regensburg, 93040 Regensburg (Germany)
[c] Environmental Monitoring Centre of Taizhou, Taizhou 318000 (China)
[d] College of Chemistry and Chemical Engineering, Xiamen University, Xiamen 361005 (China)

† Electronic Supplementary Information (ESI) available: Experimental procedures and Fig. S1-S14 See DOI: 10.1039/c000000x/

(1) J. L. Way, *Annu. Rev. Pharmacol.*, 1984, **24**, 451.
(2) Z. Xu, X. Chen, H. N. Kim and J. Yoon, *Chem. Soc. Rev.* 2010, **39**, 127.
(3) J. Ma and P. K. Dasgupta, *Anal. Chim. Acta* 2010, **673**, 117.
(4) X. Lou, D. Ou, Q. Li and Z. Li, *Chem. Commun.* 2012, **48**, 8462.
(5) (a) P. Anzenbacher, D. S. Tyson, K. Jursikova and F. N. Castellano, *J. Am. Chem. Soc.* 2002, **124**, 6232 (b) G. W. Lee, N. K. Kim and K. S. Jeong, *Org. Lett.*, 2010, **121**, 2634-2637.
(6) (a) Y. Kim, H. Zhao and F. P. Gabbai, *Angew. Chem. Int. Ed.*2009, **48**, 4957; (b) S. Madhu, S. K. Basu, S. Jadhav and M. Ravikanth, *Analyst* 2013, **138**, 299; (c) T. F. Robbins, H. Qian, X. Su, R. P. Hughes and I. Aprahamian, *Org. Lett.* 2013, **15**, 2386; (d) J. Jo, A. Olasz, C. H. Chen and D. Lee, *J. Am. Chem. Soc.* 2013, **135**, 3620; (e) M. Tomasulo and F. M. Raymo, *Org. Lett.*, 2005, **7**, 4633; (f) Y. K. Yang and J. S. Tae, *Org. Lett.*, 2006, **8**, 5721; (g) D. Cho, J. H. Kim and J. L. Sessler, *J. Am. Chem. Soc.* 2008, **130**, 12163; (h) Q. Shu, L. Birlenbach and M. Schmittel, *Inorg. Chem.* 2012, **51**, 13123; (i) X. Cheng, Y. Zhou, J. Qin and Z. Li, *Acs Appl. Mater. Interfaces* 2012, **4**, 2133.
(7) (a) X. Lou, L. Zhang, J. Qin and Z. Li, *Chem. Commun.* 2008, **44**, 5848; (b) L. Tang, N. Wang, Q. Zhang, J. Guo and R. Nandhakumar, *Tetrahedron Lett.* 2013, **54**, 536; (c) Y. Guo, X. Tang, F. Hou, J. Wu, W. Dou, W. Qin, J. Ru, G. Zhang, W. Liu and X. Yao, *Sens. Actuators, B* 2013, **181**, 202.
(8) $4Ag + 8CN^- + 2H_2O + O_2 \rightarrow 4[Ag(CN)_2]^- + 4OH^-$, $4Au + 8CN^- + 2H_2O + O_2 \rightarrow 4[Au(CN)_2]^- + 4OH^-$.
(9) (a) Y. Liu, K. Ai, X. Cheng, L. Huo and L. Lu, *Adv. Funct. Mater.* 2010, **20**, 951; (b) X. Lou, Q. Zeng, Y. Zhang, Z. Wan, J. Qin and Z. Li, *J. Mater. Chem.* 2012, **22**, 5581; (c) L. Shang and S. Dong, *Anal. Chem.* 2009, **81**, 1465; (d) L. Shang, L. Jin and S. Dong, *Chem. Commun.* 2009, **45**, 3077; (e) L. Shang, C. Qin, L. Jin, L. Wang and S. Dong, *Analyst* 2009, **134**, 1477; (f) S. C. Wei, P. H. Hsu, Y. F. Lee, Y. W. Lin and C. C. Huang, *Acs Appl. Mater. Interfaces* 2012, **4**, 2652; (g) Y. Zhai, L. Jin, P. Wang and S. Dong, *Chem. Commun.* 2011, **47**, 8268; (h) X. Lou, Y. Zhang, J. Qin and Z. Li, *Chemistry – A European Journal* 2011, **17**, 9691.

(10) (a) X. Zhang, H. Wang and Z. Su, *Langmuir* 2012, **28**, 15705; (b) L. Chuntonov, M. Bar-Sadan, L. Houben and G. Haran, *Nano Lett.* 2012, **12**, 145; (c) Y. Ma, W. Li, E. C. Cho, Z. Li, T. Yu, J. Zeng, Z. Xie and Y. Xia, *ACS Nano* 2010, **4**, 6725; (d) C. M. Gonzalez, Y. Liu and J. C. Scaiano, *J. Phys. Chem. C* 2009, **113**, 11861.

(11) C. B. Norris, P. R. Joseph, M. R. Mackiewicz and S. M. Reed, *Chem. Mater.* 2010, **22**, 3637.

(12) J. J. Du B. W. Zhu and X. D. Chen, *Small* 2013, **9**, 4104.

(13) The average thickness of silver shell was calculated using the following equation: $t=(d_1-d_2)/2$; where t, d_1 and d_2 represent the thickness of silver shell, the average diameter of Au@Ag core/shell NPs and Au NPs.

(14) Guidelines for Drinking-Water Quality, World Health Organization, Geneva, 1996.

(15) (a) S. Hajizadeh, K. Farhadi, M. Forough and R. E. Sabzi, *Anal. Methods* 2011, **3**, 2599; (b) C. Radhakumary and K. Sreenivasan, *Analyst* 2012, **137**, 5387.

(16) C. Y. Liu and W. L. Tseng, *Chem. Commun.*2011, **47**, 2550.